

Received 19 February; accepted 5 April 2000.

1. Dussan, V. E. B. & Chow, R. T. P. On the ability of drops or bubbles to stick to non-horizontal surfaces of solids. *J. Fluid Mech.* **137**, 1–29 (1983).
2. Frohn, A. & Roth, R. *Dynamics of Droplets* (Springer, Berlin, 2000).
3. Perez, M. *et al.* Oscillation of liquid drops under gravity: influence of shape on the resonance frequency. *Europhys. Lett.* **47**, 189–195 (1999).
4. Mahadevan, L. & Pomeau, Y. Rolling droplets. *Phys. Fluids* **11**, 2449–2453 (1999).
5. Onda, T., Shibuichi, S., Satoh, N. & Tsujii, K. Super water-repellent fractal surfaces. *Langmuir* **12**, 2125–2127 (1996).
6. Taylor, G. I. & Michael, D. H. On making holes in a sheet of fluid. *J. Fluid Mech.* **58**, 625–639 (1973).
7. Richard, D. & Quéré, D. Drops rolling on a tilted non-wettable solid. *Europhys. Lett.* **48**, 286–291 (1999).
8. Wang, T. G. *et al.* Bifurcation of rotating liquid drops: results from USML-1 experiments in space. *J. Fluid Mech.* **276**, 389–403 (1994).
9. Lee, C. P. *et al.* Equilibrium of liquid drops under the effects of rotation and acoustic flattening: results from USML-2 experiments in space. *J. Fluid Mech.* **354**, 43–67 (1998).
10. Brown, R. A. & Scriven, L. E. The shape and stability of rotating liquid drops. *Proc. R. Soc. Lond. A* **371**, 351–367 (1980).
11. Brown, R. A. & Scriven, L. E. New class of asymmetric shapes of rotating liquid drops. *Phys. Rev. Lett.* **45**, 180–183 (1980).
12. Rayleigh, Lord The equilibrium of revolving liquid under capillary force. *Phil. Mag.* **28**, 161–170 (1914).
13. Plateau, J. A. F. Experimental and theoretical researches on the figures of equilibrium of a liquid mass withdrawn from the action of gravity. *Annu. Rep. Board Regents Smithsonian. Inst.* 207–285 (1863).
14. Chandrasekhar, S. The stability of a rotating liquid drop. *Proc. R. Soc. Lond. A* **286**, 1–26 (1965).

Acknowledgements

We thank J. Bico and D. Richard for silanization of lycopodium grains and the achievement of a first series of liquid marbles, C. Clanet for help with high-speed pictures and for discussions, and P.-G. de Gennes for discussions and encouragement.

Correspondence and requests for materials should be addressed to D.Q. (e-mail: quere@ext.jussieu.fr).

Decreasing overflow from the Nordic seas into the Atlantic Ocean through the Faroe Bank channel since 1950

Bogi Hansen*, William R. Turrell† & Svein Østerhus‡

* Faroese Fisheries Laboratory, PO Box 3051, FO-110 Tórshavn, Faroe Islands
 † FRS Marine Laboratory, PO Box 101, Aberdeen AB11 9DB, UK
 ‡ Bjerknes Centre for Climate Research and Geophysical Institute, N-5024 Bergen, Norway

The overflow of cold, dense water from the Nordic seas, across the Greenland–Scotland ridge¹ and into the Atlantic Ocean is the main source for the deep water of the North Atlantic Ocean². This flow also helps drive the inflow of warm, saline surface water into the Nordic seas¹. The Faroe Bank channel is the deepest path across the ridge, and the deep flow through this channel accounts for about one-third of the total overflow^{1,2}. Previous work has demonstrated that the overflow has become warmer and less saline^{3,4} over time. Here we show, using direct measurements and historical hydrographic data, that the volume flux of the Faroe Bank channel overflow has also decreased. Estimating the volume flux conservatively, we find a decrease by at least 20 per cent relative to 1950. If this reduction in deep flow from the Nordic seas is not compensated by increased flow from other sources, it implies a weakened global thermohaline circulation and reduced inflow of Atlantic water to the Nordic seas.

The Nordic seas and the Arctic Ocean are dominated by cold water below about 500 m depth—the typical sill depth of the Greenland–Scotland ridge (Fig. 1). The overflow of this water across the Greenland–Scotland ridge into the North Atlantic is the most important source for North Atlantic Deep Water²

(NADW), and any assessment of past or future variation in the global thermohaline circulation will depend critically on assessing the variation of this overflow. About half of the overflow passes through the Denmark Strait, while the rest crosses the ridge in the Iceland–Scotland region², mainly through the Faroese channels—consisting of the Faroe–Shetland channel leading to the Faroe Bank channel (Fig. 1b).

The Faroe Bank channel has a sill depth of around 840 m, and the deepest parts of the channel are constantly filled with cold overflow water flowing into the Atlantic with average velocities exceeding 1 m s⁻¹ in the core (Fig. 2). Since November 1995, an upward-looking acoustic Doppler current profiler (ADCP) has been moored at the sill of the channel and has measured the velocity profile almost continuously. From these measurements, initiated in the ‘Nordic WOCE’ project, the flux of water colder than 3 °C was estimated⁵ to be 1.9 Sv (1 Sv = 10⁶ m³ s⁻¹), which is fairly consistent with previous estimates^{6,7}. This flux includes the overflow waters, but also some entrained Atlantic water. To avoid influence from the entrained water, we focus on the well defined overflow, colder than +0.3 °C and with densities (σ_t) in excess of 28.0. From November 1995 to June 2000, the ADCP measurements indicate a weakening of this overflow flux of 2–4% per year (Fig. 3), which is significantly different from zero ($P < 0.001$).

Direct current measurements give the most reliable estimate of the overflow flux through the Faroe Bank channel, but for information on long-term variations we are restricted to more indirect methods. Historical hydrographic data may be used for this purpose if they can be related to the overflow on a theoretically sound basis. In the

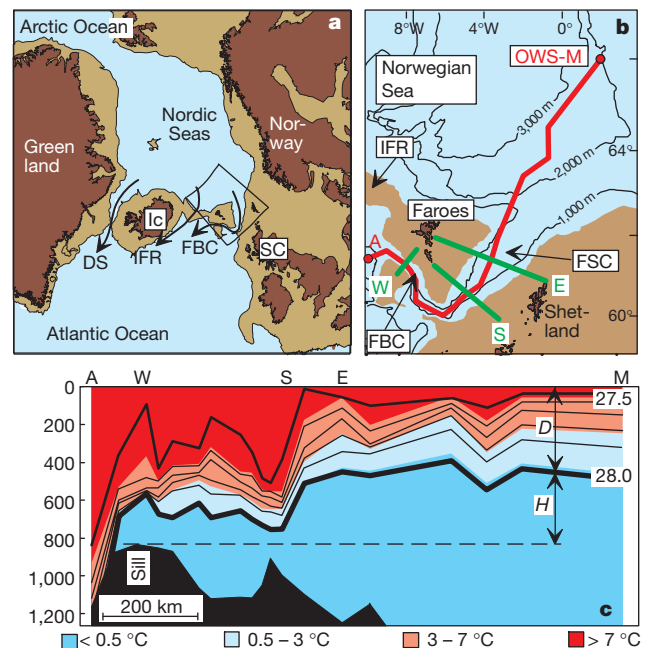


Figure 1 Topography and temperature change across the Greenland–Scotland ridge (light-brown areas are shallower than 500 m). **a**, Map of the Greenland–Iceland (Ic)–Scotland (Sc) region. Black arrows show overflow paths through the Denmark Strait (DS), over the Iceland–Faroe ridge (IFR), and through the Faroe Bank channel (FBC). **b**, Bottom topography of the study area (indicated by box in **a**) and location of a longitudinal (red line from A to OWS-M) and three transverse (green lines labelled W, S and E) standard hydrographic sections. Arrows indicate the Iceland–Faroe ridge (IFR), the Faroe–Shetland channel (FSC), and the Faroe Bank channel (FBC). **c**, Temperature (colour shading) and σ_t isopycnals (contours) along the longitudinal section, based on CTD (conductivity–temperature–depth) observations from RV *Magnus Heinason* in May–August 1991 and observations at OWS-M in the same period. The definition of the interface depth D and height H is illustrated.

steady state, the equations of motion may, to a first approximation, be integrated horizontally along the channel axis (x) and vertically (z) over the overflow layer to give:

$$\int \frac{1}{2} \rho U^2 dz - \int (\tau_{\text{top}} - \tau_{\text{bottom}}) dx = \int (p_u - p_s) dz = \Delta P \quad (1)$$

where U is the along-channel velocity at the sill, τ the frictional stress, and $(p_u - p_s)$ the difference between the upstream (p_u) and downstream, or sill (p_s), pressure. In the open Atlantic, outside the exit of the channel, the density above sill level referred to atmospheric pressure (ρ_0) is fairly constant. In the channel, the density structure is often approximated by a two-layer system, but at the upstream end it is better described as increasing linearly from ρ_0 in the surface to $\rho_0 + \Delta\rho$ (referred to atmospheric pressure) at the depth (D) of the interface, and then remaining constant through the overflow layer of height H (Fig. 1c). In this approximation, the integrated pressure difference is given by $\Delta P = (1/2)\Delta\rho gH(D + H)$.

The vertically integrated pressure difference between both ends of the channel (ΔP) is the driving force for the overflow, and because the frictional stress increases with velocity, equation (1) implies the intuitively obvious statement that the overflow flux is a monotonically increasing function of ΔP and hence also of H . This is the basis for the main conclusion of this Letter, as we infer a changing overflow flux (q) from an observed change in H . Quantitative relationships between q and H have been derived from analytical models^{6,8}, and generally imply that q is proportional to H raised to the power 3/2 or 2 depending on channel geometry. These models ignore friction, however, which is not permissible for the Faroe Bank channel^{7,9}. They also assume a pure two-layer structure. Using the more realistic expression for ΔP given above and assuming a narrow channel of rectangular cross-section, with constant velocity in the overflow layer and the interface height at the sill proportional to H , equation (1) implies:

$$q = \alpha H^n \quad (2)$$

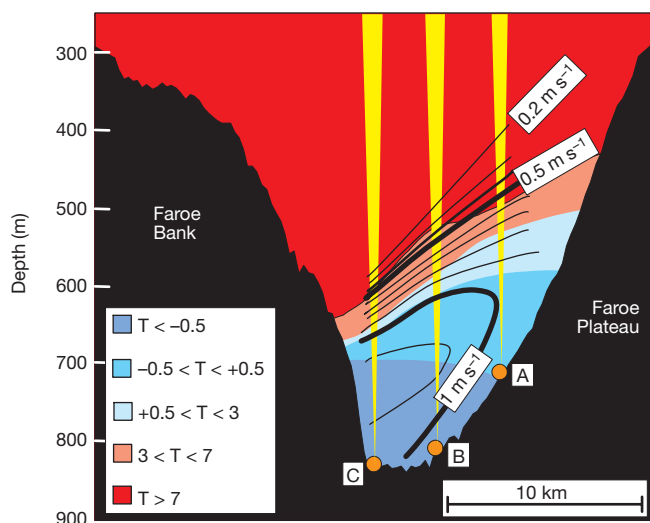


Figure 2 Section across the Faroe Bank channel (W in Fig. 1b) at the sill showing the temperature and velocity of the water below 250 m depth. Colour shading indicates the temperature distribution (in °C) observed on a cruise in September 1998. Contours show the average distribution of the along-channel velocity towards the northwest (positive into the paper) in the period July–September 1998 based on observations from three moored ADCPs (A, B and C) deployed during the VEINS project. Yellow cones illustrate sound beams. Assuming that the cross-sectional variation of velocity determined by this experiment is representative, volume flux below a given isotherm can be calculated from the central mooring alone.

where α is a constant, and $n = 1$ in the case where the first term (inertia) on the left hand side of equation (1) dominates, and $n = 3/2$ if the second term (friction) dominates and is quadratic in velocity. We use the constant-density level ($\sigma_t = 28.0$ isopycnal) to define the interface, and H is thus the height of this isopycnal above sill level (Fig. 1c).

Mesoscale activity deforms the isopycnals on timescales of days (Fig. 1c), which necessitates frequently sampled data. Such data are available at Ocean Weather Station M (OWS-M, Fig. 1b), where temperature and salinity have been observed since 1948 with several profiles a month¹⁰. Using these data, we established a time series of the depth of the $\sigma_t = 28.0$ isopycnal at OWS-M which exhibits a persistent deepening trend from 1950 to 1999 (Fig. 4). The annual depth increase was 1.05 ± 0.15 m (average \pm standard error), which is statistically different from zero at a high level of significance ($P < 0.001$). This implies that the overflow also decreased over the 1950–99 period. Using equation (2), we find a decrease by 20% ($n = 1$) or by 26% ($n = 3/2$) relative to 1950.

A number of critical questions may be raised about the method and the associated assumptions. These are assessed in the Methods section, where we argue that they are unlikely to affect the basic conclusion of a weakened overflow flux. Fortunately, there is a way to test the assumption of a direct link between overflow flux through the Faroe Bank channel and interface height at OWS-M, because there is a period from November 1995 to January 1999 when simultaneous measurements exist of isopycnal depth at OWS-M and directly measured overflow flux in the Faroe Bank channel.

To compare these two sets of observations, we converted monthly interface depths at OWS-M to overflow flux using equation (2), smoothed them, and plotted them together with the flux computed from the ADCP measurements for the common period (Fig. 3). The two curves in Fig. 3 are not identical, but they show similar behaviour even at seasonal and interannual timescales as regards typical amplitudes and trends. This confirms that changes in the interface height at OWS-M reflect changes in overflow forcing, and supports our conclusion that the Faroe Bank channel overflow has decreased since 1950. This conclusion applies to water colder than 0.3°C , which accounts for about two-thirds of the total overflow flux (defined as water colder than 3°C). The remainder has densities ranging down to $\sigma_t = 27.8$, and this isopycnal has also deepened at OWS-M at similar rates since 1950. Thus, a decrease of the total Faroe Bank Channel overflow by about 0.5 Sv since 1950 is a conservative estimate.

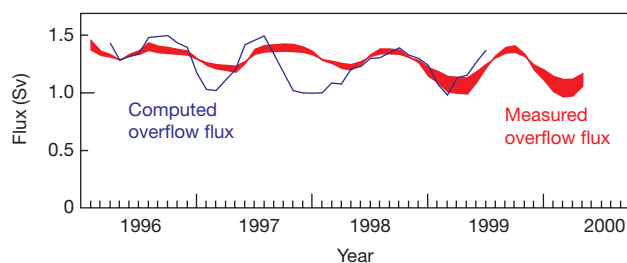


Figure 3 The flux of water below the 0.3°C isotherm through the Faroe Bank channel. Red curve, as measured by moored ADCPs; blue curve, as computed from OWS-M interface depth. Both series have been filtered using 5-month running means. The width of the red curve illustrates the uncertainty of the flux calculations due to a lack of information on the vertical isotherm movement in response to velocity changes⁵. The decreasing trend is estimated to be 2% or 4% per year, depending on the assumptions. The blue curve was computed from equation (2) with $n = 1$; α was determined by the average overflow flux and upstream interface height, and lagged by 8 months because independent hydrographic observations (see Methods) indicate that there is an 8-month delay in the interface height variations from OWS-M to the Faroe Bank channel.

Previous investigations^{3,4} have demonstrated a change in the composition of the Faroe Bank channel overflow that implies a reduction of the average density of the overflow water since the mid-1970s. Up to now, there was no observational evidence for changes in the overflow flux, but it has been argued³ that less-dense overflow water would entrain less ambient water in the Atlantic after leaving the channel. This would imply a reduced flux of the mixture of overflow water and entrained water feeding into the NADW. Our observed reduction of the overflow flux comes in addition to this. The Faroe Bank channel overflow has become less intensive and less dense, and both these effects have acted to reduce the supply of dense water to NADW.

The implications of our observed decrease of Faroe Bank channel flux depend on the behaviour of the other overflow sources. East of Iceland, the only source of sufficient magnitude to affect our conclusion is the overflow over the Iceland–Faroe ridge¹ (Fig. 1). The volume flux of this source can also be expected to decrease with a deepening interface in the southern Norwegian Sea. Thus, the total Iceland–Scotland overflow has probably decreased since 1950. In the Denmark Strait, analysis of hydrographic data since 1950 has indicated decadal variability in the overflow there¹, but this was based on the geostrophic method which is questionable in slope regions¹. Direct current measurements of the Denmark Strait overflow are more recent, but they show “surprisingly little evidence of variability over longer periods (months, seasons, years)”¹².

Thus, we cannot exclude the possibility of an increased Denmark Strait overflow that compensates for our observed decrease of Iceland–Scotland overflow, but we find no evidence for it. It has been shown that the formation of deep water by convection in the Greenland Sea has decreased since around 1970¹³, but that decrease might well have been compensated by a shift to more intensive formation of intermediate water¹. Unless there is an unobserved increase in flux from the Denmark Strait, our results suggest a reduction in the total formation of deep and intermediate waters north of the Greenland–Scotland ridge. This is consistent with predictions from global coupled atmosphere–ocean models as a consequence of an increase in anthropogenic greenhouse gases¹⁴.

The consequences for NADW production depend on entrainment as well as convection in the Labrador Sea, but, in any case, our results imply a reduced input of dense water from the Iceland–Scotland region and hence a reduced forcing of the meridional overturning from this overflow component.

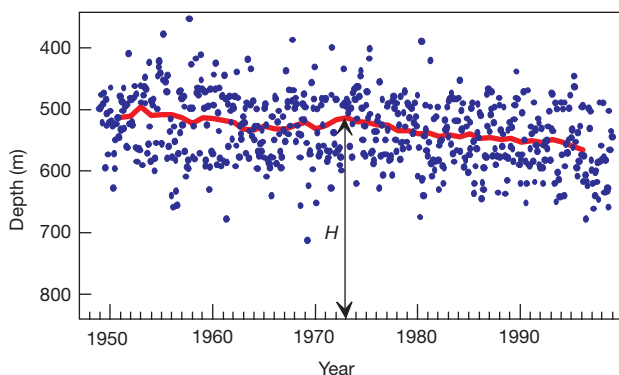


Figure 4 Depth of the $\sigma_t = 28.0$ isopycnal at OWS-M. Blue dots, monthly means. Red curve, 5-year running mean. Around 1970, the steady deepening of the interface seems to have been halted or even temporarily reversed at a time of intense deep-water formation in the Greenland Sea¹³. We note that during the decade 1990–99, the deepening of the $\sigma_t = 28.0$ isopycnal was about twice the typical decadal deepening for the whole period, which brings it closer to the trend measured by the ADCPs since 1995 (Fig. 3). H is the height of the isopycnal above sill level.

Our results also have implications for the Atlantic inflow to the Nordic seas. According to recent estimates¹, this inflow is mainly returned to the Atlantic in the overflows (75%) rather than in the surface flow (25%). This implies that the barotropic pressure gradient induced by the overflow is an important part of the driving force for the inflow¹. A reduced overflow can therefore be expected to lead to a reduced Atlantic inflow of a similar magnitude. The heat transported by the Atlantic inflow gives rise to the exceptionally mild climate of northwestern Europe¹⁵, and a reduction of the inflow will have a regional cooling effect that counteracts the global warming trend. As yet, direct flux measurements of the Atlantic inflow¹ are of too short duration to establish long-term trends, but reports of cooling and freshening in the Norwegian Sea¹⁶—and of decreasing air temperatures in some of the regions most affected by the inflow¹⁷—could perhaps be partly explained by a reduced inflow. □

Methods

Interface depth

The depth of the $\sigma_t = 28.0$ isopycnal at OWS-M was determined by linear interpolation between the standard observational depths: 400 m, 500 m, 600 m and 800 m. Thus, the depth interval between observations is twice the magnitude of the deepening trend. This, as well as mesoscale activity, argues that caution should be used in interpreting small isopycnal depth changes. We find, however, that the observed long-term deepening of 50 m is too large to be a statistical artefact. Spurious trends due to changing methodology, especially in salinity analysis, may also be discounted because they would have shown up also at deeper levels (beyond 1,500 m depth)—and they do not.

To establish the propagation of interface changes from OWS-M to the Faroe Bank channel, the timing of the seasonal maximum height of the $\sigma_t = 28.0$ isopycnal above sill depth was determined. At OWS-M, monthly average depths were fitted by a sinusoidal function with annual period added to a linear trend, and the maximal height was found to occur in January. In the Faroese channels, a similar analysis was performed using hydrographic observations from Scottish and Faroese research vessel cruises on three standard sections (Fig. 1b). There the maximal height was found to occur in June on section E and in August–September on sections S and W. This corresponds to an 8-month delay from OWS-M to the Faroe Bank channel.

Potential sources of error

It could be argued that the integrated pressure difference depends on other things rather than solely on the upstream interface height. One of these is the density in the Atlantic. We have examined a large number of stations from the 1950–99 period, obtained from the ICES (International Council for the Exploration of the Sea) Data Bank and the national Faroese data archive. Decadal averages of σ_t for each of the five decades ranged between 27.49 and 27.51 for the layer of depth 500–800 m. This verifies that the Atlantic waters just outside the exit of the channel have remained constant in density; but changes in the Norwegian Sea above the interface may also affect the horizontal pressure gradient at depth. The observations from the upper layers at OWS-M show that density in the upper layers has decreased slightly throughout most of the period, but this would tend to magnify the effect of a deepening interface on the overflow flux, not counteract it.

A difference in sea-level height between the Atlantic and the Norwegian Sea induces a barotropic pressure gradient. A systematic change in this could have offset the changing baroclinic pressure gradient implied by Fig. 4. Except for changing overflows, the only likely mechanism to induce a changing barotropic pressure gradient is the wind, and there certainly have been systematic changes in the wind—as documented by the well-known changes in the North Atlantic Oscillation (NAO) index¹⁸. These changes in the wind-forcing are, however, characterized by strengthening multi-decadal oscillations which are not seen in Fig. 4.

Using the interface height at OWS-M to reflect the overflow forcing presupposes that internal circulation in the Norwegian Sea does not change the interface depth between OWS-M and the channel entrance too much. Using high-quality data, available since 1994, we determined the average depth of the $\sigma_t = 28.0$ isopycnal from section E (Fig. 1b), close to the channel entrance, to be 562 ± 19 m (average \pm standard error) in the period 1994–99. In the same period, the depth of this isopycnal at OWS-M was almost identical (565 ± 7 m). This argues that changes of the interface height between OWS-M and the channel entrance due to internal circulation are small compared to the 50-m change observed (Fig. 4).

Received 24 November 2000; accepted 19 April 2001.

- Hansen, B. & Østerhus, S. North Atlantic - Nordic Seas exchanges. *Prog. Oceanogr.* **45**, 109–208 (2000).
- Dickson, R. R. & Brown, J. The production of North Atlantic Deep Water: Sources, rates and pathways. *J. Geophys. Res.* **99**, 12319–12341 (1994).
- Turrell, W. R., Slessor, G., Adams, R. D., Payne, R. & Gillibrand, P. A. Decadal variability in the composition of Faroe Shetland Channel Bottom Water. *Deep-Sea Res.* **46**, 1–25 (1999).
- Hansen, B. & Kristiansen, R. Variations of the Faroe Bank Channel overflow. *Rit Fiskid.* **16**, 13–21 (1999).

5. Østerhus, S., Hansen, B., Kristiansen, R. & Lundberg, P. The Overflow through the Faroe Bank Channel. *Int. WOCE Newsl.* **35**, 35–37 (1999).
6. Borenäs, K. M. & Lundberg, P. A. On the deep-water flow through the Faroe Bank Channel. *J. Geophys. Res.* **93**, 1281–1292 (1988).
7. Saunders, P. M. Cold outflow from the Faroe Bank Channel. *J. Phys. Oceanogr.* **20**, 29–43 (1990).
8. Whitehead, J. A. Topographic control of oceanic flows in deep passages and straits. *Rev. Geophys.* **36**, 423–440 (1998).
9. Crease, J. The flow of Norwegian Sea Water through the Faroe Bank Channel. *Deep-Sea Res.* **12**, 143–150 (1965).
10. Østerhus, S. & Gammelsrød, T. The abyss of the Nordic Seas is warming. *J. Clim.* **12**, 3297–3304 (1999).
11. Bacon, S. Decadal variability in the outflow from the Nordic Seas to the deep Atlantic Ocean. *Nature* **394**, 871–874 (1998).
12. Dickson, R. R., Meincke, J., Vassie, I., Jungclauss, J. & Østerhus, S. Possible predictability in overflow from the Denmark Strait. *Nature* **397**, 243–246 (1999).
13. Clarke, R. A., Swift, J. H., Reid, J. L. & Koltermann, K. P. The formation of Greenland Sea deep water: Double diffusion or deep convection? *Deep-Sea Res.* **37**, 1385–1424 (1990).
14. Rahmstorf, S. Shifting seas in the greenhouse? *Nature* **399**, 523–524 (1999).
15. Rahmstorf, S. & Ganopolski, A. Long-term global warming scenarios computed with an efficient coupled climate model. *Clim. Change* **43**, 353–367 (1999).
16. Blindheim, J. et al. Upper layer cooling and freshening in the Norwegian Sea in relation to atmospheric forcing. *Deep-Sea Res.* **47**, 655–680 (2000).
17. Cappelen, J. & Laursen, E. V. *The Climate of the Faroe Islands* (Danish Meteorological Institute Technical Report 98-14, Copenhagen, 1998).
18. Hurrell, J. W. Decadal trends in the North Atlantic Oscillation: Regional temperatures and precipitation. *Science* **269**, 676–679 (1995).

Acknowledgements

The 'Nordic WOCE' project was funded by the Nordic Environmental Research Programme for 1993–97, and by Nordic national research councils. The 'VEINS' project was supported by the MAST IV Programme of the European Community.

Correspondence and requests for material should be addressed to B.H. (e-mail: bogihan@frs.fo).

Metamorphic core complex formation by density inversion and lower-crust extrusion

Fernando Martinez*, Andrew M. Goodliffe* & Brian Taylor†

*Hawaii Institute of Geophysics and Planetology, †Department of Geology and Geophysics, School of Ocean and Earth Science and Technology, University of Hawaii, Honolulu, Hawaii 96822, USA

Metamorphic core complexes are domal uplifts of metamorphic and plutonic rocks bounded by shear zones that separate them from unmetamorphosed cover rocks¹. Interpretations of how these features form are varied and controversial, and include models involving extension on low-angle normal faults², plutonic intrusions³ and flexural rotation of initially high-angle normal faults⁴. The D'Entrecasteaux islands of Papua New Guinea are actively forming metamorphic core complexes located within a continental rift that laterally evolves to sea-floor spreading⁵. The continental rifting is recent (since ~6 Myr ago)⁵, seismogenic⁶ and occurring at a rapid rate (~25 mm yr⁻¹)⁵. Here we present evidence—based on isostatic modelling, geological data and heat-flow measurements—that the D'Entrecasteaux core complexes accommodate extension through the vertical extrusion of ductile lower-crust material, driven by a crustal density inversion. Although buoyant extrusion is accentuated in this region by the geological structure present—which consists of dense ophiolite overlaying less-dense continental crust—this mechanism may be generally applicable to regions where thermal expansion lowers crustal density with depth.

The tectonic evolution of eastern Papua New Guinea created a crustal density inversion central to the proposed mechanism of core complex formation. The region of the palaeo-Papuan peninsula

west of 153° 20' E including the D'Entrecasteaux islands and the Goodenough basin (Fig. 1) originated in Palaeogene times as an intra-oceanic arc accommodating northerly directed subduction^{7,8}. The subducting plate included a continental fragment, the Papuan plateau, which had become detached from the margin of Australia by the opening of the Coral Sea basin⁹. When the Papuan plateau encountered the trench it was partially subducted⁹, and island arc ophiolite was obducted onto it^{7,10}. Northward subduction ceased and subduction later reversed¹¹. Southward subduction along the Trobriand trough led to arc magmatism throughout Miocene–Holocene times¹².

Sea-floor spreading in the easternmost Woodlark basin initiated by 6 Myr ago, and rifting around the D'Entrecasteaux islands had begun by Pliocene times¹² (Fig. 1). A seismic receiver function study¹³ indicates that the crust thins from 32–43 km beneath the Papuan peninsula to 20–26 km beneath the Goodenough basin and D'Entrecasteaux islands. On the D'Entrecasteaux islands, pressure–

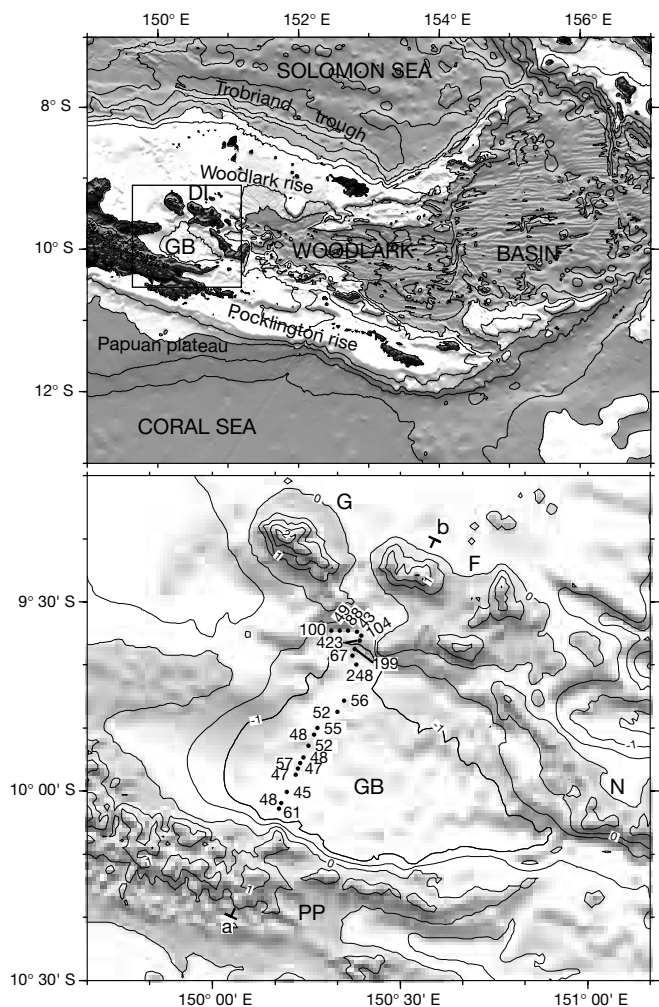


Figure 1 The eastern Papuan peninsula has been undergoing extension since at least 6 Myr ago. Top, sea-floor spreading in the oceanic Woodlark basin split the palaeo-peninsula to form the Woodlark and Pocklington rises as rifted margins. Extension decreases westwards. Continental rifting continues in the Goodenough basin and D'Entrecasteaux islands. Bottom, details of the study area indicated by the box in the top panel. Shown are the locations of the heat-flow measurements and their values (in mW m⁻²) uncorrected for sedimentation. Also shown are bathymetry and topography with contours at 500-m intervals annotated every kilometre. Abbreviations: DI, D'Entrecasteaux islands; GB, Goodenough basin; G, Goodenough island; F, Fergusson island; N, Normanby island; PP, Papuan peninsula. 'a–b' indicates modelled section shown in Fig. 4.